



OPEN ACCESS

EDITED BY

Faryal Idrees,
University of the Punjab, Pakistan

REVIEWED BY

Sadia Iqbal,
The Women University, Multan, Pakistan
Athar Javed,
University of the Punjab, Pakistan

*CORRESPONDENCE

Xiangbing Gong,
✉ xbgong@csust.edu.cn

RECEIVED 14 October 2023

ACCEPTED 11 January 2024

PUBLISHED 24 January 2024

CITATION

Huang P, Chen F, Cai M, Gong X, Huang X,
Jiang Y and Liu Z (2024), Multi-functional
composite coating based on the dual effects
of cooling and exhaust gas degradation.
Front. Mater. 11:1321429.
doi: 10.3389/fmats.2024.1321429

COPYRIGHT

© 2024 Huang, Chen, Cai, Gong, Huang,
Jiang and Liu. This is an open-access article
distributed under the terms of the [Creative
Commons Attribution License \(CC BY\)](#). The
use, distribution or reproduction in other
forums is permitted, provided the original
author(s) and the copyright owner(s) are
credited and that the original publication in
this journal is cited, in accordance with
accepted academic practice. No use,
distribution or reproduction is permitted
which does not comply with these terms.

Multi-functional composite coating based on the dual effects of cooling and exhaust gas degradation

Peng Huang¹, Feng Chen¹, Mingming Cai¹, Xiangbing Gong^{2*},
Xue Huang², Yu Jiang² and Ziming Liu²

¹Guangzhou Expressway Company, Guangzhou, China, ²School of Traffic and Transportation Engineering, Changsha University of Science and Technology, Changsha, China

High-temperature hazards of asphalt pavement and pollution from car exhaust are two major problems that need to be solved in road construction. In this paper, a multifunctional composite coating has been prepared from the perspective of reducing road temperature and car exhaust degradation. The principle of heat-reflecting coating is used to reduce the road surface temperature. At the same time, the TiO₂ aqueous solution with photocatalytic degradation effect is added to the heat-reflective coating material to achieve the purpose of degrading automobile exhaust degradation, creating a new type of multifunctional coating that has both cooling and exhaust degradation effects. In addition, by changing the amount of carbon black, a multi-functional coating with the best coloring is selected, so that it has better functionality and has the most suitable shade for the road surface. Finally, the cooling effect and the exhaust gas reduction effect are examined through indoor and outdoor tests and the slip resistance of the coating is tested using the pendulum method. The results show that the functional coating group has a certain ability of cooling and exhaust gas degradation compared to the normal control group without coating. For the functional coating group with different carbon black content, the functional coating (G2) with 0.9% carbon black content has the strongest overall functionality. The cooling and exhaust gas reduction effects proved to be the best. The surface cooling rate is 5.4°C, while the internal cooling rate is 4.3°C. The cumulative degradation efficiency of CO and NO is found to be 27.77%, and 73.75%, respectively.

KEYWORDS

multi-functional composite coating, heat-reflective coating, photocatalytic degradation, cool pavement, urban heat island effect (UHI)

1 Introduction

Asphalt pavement is the most widely used form of pavement in highways and urban road systems due to its advantages, and its application proportion is far greater than that of cement concrete pavement. However, asphalt pavement is black and its absorption rate of solar radiation can be as high as 85%–95% (Lei, 2010; Gong et al., 2020). Because of the strong temperature dependence, the persistently high temperature in summer leads to an increase in the temperature of the asphalt pavement, which is susceptible to rutting, shifting, oiling, and congestion (Si et al., 2018; Cheng et al., 2020).

At the same time, with the continuous improvement of living standards and quality of life, the number of national motor vehicles and mileage on highways have also increased rapidly year by year. While this facilitates people's transportation and travel, the environment is inevitably seriously polluted by the large amounts of automobile exhaust, which has become one of the major environmental problems of road transportation (Zhang et al., 2018; Cui et al., 2020).

The risk of high temperature on asphalt surfaces is mainly expressed in two aspects: rutting and the heat island effect. Rutting is the permanent deformation of the road structure layer under the repeated impact of vehicle load. Due to the softening of asphalt under high-temperature conditions, displacement of asphalt mixture occurs. The heat island effect refers to the phenomenon that the temperature inside the city is significantly higher than the temperature outside the city. With increasing urbanization, a series of ecological and environmental problems have emerged that have negatively impacted people's health and quality of life (Wang et al., 2014; Debbage and Shepherd, 2015; Suszanowicz and Kolasa-Wiecek, 2019). Among them, the impact of urban temperature rise caused by the heat island effect is particularly serious. According to the data, the annual average temperature in the city is 2°C higher than in the suburbs, and in the hot summer, the temperature difference between the indoors and outdoors is up to 10°C (Mathew et al., 2018; Zhang et al., 2020; Kang et al., 2022). At present, to slow down the heat island effect, a series of remediation measures such as Sponge City and increasing green space coverage have been adopted, but they only achieved certain results in the local area, and did not fundamentally solve the problem of high temperature impacts caused by the heat island effect (Lin et al., 2019; Wang et al., 2019). From a road construction perspective, in order to mitigate the negative effects of solar radiation on asphalt pavements, it is necessary to reduce the thermal effect of the road. By improving the heat exchange between the asphalt pavement and the natural environment, the hydrothermal circulation system changes the heat transfer system. Nowadays, it has formed a heat-shielded pavement, a water-retaining pavement, thermal resistance pavement and a permeable pavement based on low heat absorption pavement. The study finds that the water stability and durability of the water-retaining asphalt pavement are insufficient, which has a negative impact on the structural layer of the asphalt pavement (Geng et al., 2019; Shimazaki et al., 2022). The cooling effect of the thermal resistance pavement is not good, and its cooling effect is mainly reflected in the middle and lower layers of the pavement structure, which does not have a sufficient mitigation effect on the urban heat island effect (Du et al., 2020; Zhang et al., 2022). Permeable pavements require the addition of many coarse aggregates and high-viscosity asphalt, but there is still a risk of rutting (Liu et al., 2018; Kia et al., 2021). The heat-shielding pavement uses the principle of reflecting solar radiation and uses the heat-reflecting coating technology to change the absorption of solar radiation by the asphalt pavement, so as to achieve the cooling effect of the pavement. This type of pavement has a certain cooling effect, but attention must be paid to slip resistance (Dalapati et al., 2016; Chulkov et al., 2019; Si et al., 2022; Gao et al., 2023). Synnefa et al. have compared the cooling effect of heat-reflecting coatings made from white, green, red and gray pigments. The results show that the reflectivity of the coatings of the four colors were all higher than that of the ordinary

pavement, and the maximum temperature drop reached 12°C (Synnefa et al., 2011). Guntor N AA uses epoxy resin and hardener as base material, crushes brick and tile waste as fine aggregate, sand through 0.5–2 mm sieve as filler, and mixes broken tiles, sand and base material in the same mass ratio to prepare cooling materials (Guntor et al., 2014). It is brushed onto the asphalt surface according to the coating amount of 1.2 kg/m². After a week of cooling tests, the results show that the reflectivity of the pavement can be increased by 41% and the solar radiation can be reduced by 37.06%. In addition, the pollution problem caused by car exhaust has always been a problem. Its harmful components primarily include hydrocarbons, nitrogen oxides, etc., which cause serious harm to human health. As the next source of contact after the exhaust emission of motor vehicles, the road is about 30 cm away from the exhaust emission position. Therefore, this is obviously the most direct way, using the road surface as an entry point, and applying photocatalytic technology to the road surface treatment to achieve rapid exhaust gas degradation is considered an effective means of solving the problem of exhaust pollution (Jiang and Yu, 2020). For this reason, researchers at home and abroad have carried out numerous research works and found that titanium dioxide has strong photocatalytic degradation ability for pollutants (Maury-Ramirez et al., 2013). It can capture certain photon energy and reduce nitrogen hydrides and hydrocarbons in car exhaust into harmless substances such as water, carbon dioxide and salt. Xu et al. (2018) investigated the effect of recycled aggregate on the photocatalytic performance of nano-TiO₂ concrete. The results show that recycled aggregates coated with nano-TiO₂ significantly improve the photocatalytic performance of nano-TiO₂ concrete (Xu et al., 2018). Yu et al. studied the influence of light intensity on the photocatalytic performance of nano-TiO₂ using visible light as the indoor light source. The results showed that the efficiency of NO_x removal by nano-TiO₂ increased with increasing light intensity (Brouwers, 2009).

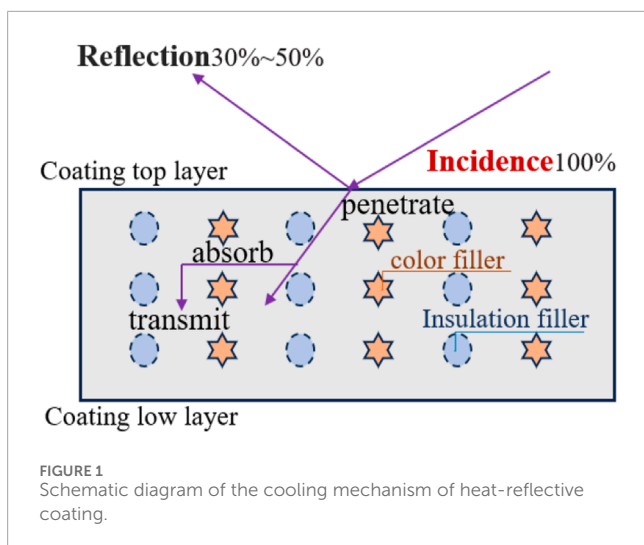
In summary, the high temperature of asphalt pavement is the main cause of rutting and urban heat island effect. At the same time, with the increasing number of cars, car exhaust fumes have caused a significant burden on human health and the natural environment. At present, research at home and abroad only focuses on one of the problems, and the function is relatively simple and not economical. Therefore, a multifunctional composite asphalt pavement structure with dual effects of temperature regulation and exhaust gas degradation is proposed in this paper. The road temperature is reduced by using heat reflective coating technology, and the catalytic aqueous solution of titanium dioxide is added to the heat reflective coating material for photocatalytic degradation to achieve the purpose of reducing automobile exhaust pollution.

2 Materials and experimental design

2.1 Material selection mechanism

2.1.1 Cooling mechanism of heat-reflective coating

Compared with ordinary pavement, the surface layer of heat reflective pavement is covered with a film containing base material, pigments and fillers, and heat-insulating fillers. The upper layer of the coating film can reflect part of the incident light to the



external environment, while the other part of the heat enters the interior of the coating film and comes into contact with the heat-insulating filler, such as a hollow microsphere. Due to the poor thermal conductivity of the gas inside the hollow microsphere, it can block heat transfer to the lower layer. At this point, the solar radiation heat is partially reflected by the coating, the blocking part and the absorbing part, and finally the remaining part is transmitted downward, which can reduce the absorption and accumulation of heat by the asphalt pavement to achieve the purpose of cooling. The cooling mechanism of the heat-reflective coating is shown in Figure 1.

2.1.2 Degradation mechanism of exhaust gas by photocatalytic material

Currently, the most commonly used material in asphalt exhaust degradation is nanotitanium dioxide. Titanium dioxide (TiO_2) has three crystal forms: brookite, anatase and rutile. Based on the principle of photocatalysis, when the light energy of the photocatalytic material is greater than the energy of the band gap, the electrons in the valence band change to the conduction band, leaving holes in the valence band and forming electron-hole pairs. Secondly, the O_2 adsorbed on the surface of the catalyst captures electrons and forms superoxide radicals ($\cdot\text{O}_2^-$). The hole oxidation of water (H_2O) or hydroxide (OH^-) adsorbed on the surface of the catalyst is a hydroxyl radical ($\cdot\text{OH}$). Finally, both $\cdot\text{O}_2^-$ and $\cdot\text{OH}$ are strongly oxidizing, and most organic substances can be oxidized to CO_2 and H_2O . When the photocatalytic material is exposed to photons with energy higher than its band gap, electron transfer occurs. Finally, hydroxyl radicals ($\cdot\text{OH}$) and superoxide radical ($\cdot\text{O}_2^-$) form an oxidation group on the surface of the catalytic material. The oxidation group has strong redox ability, which can convert harmful components CO , HC and NO_x in car exhaust into harmless water, CO_2 , and other harmless substances.

2.1.3 Selection mechanism of composite coating material

In general, organic/inorganic composite materials can not only retain the flexibility, plasticity and light transmittance of

organic polymer materials, but also exploit the advantages of non-flammability, strong weather resistance, good wear resistance and high hardness of inorganic materials. Aluminum sol and silica sol are commonly used inorganic raw materials in composite materials. In this study, silica sol is selected as an inorganic raw material. Since organic and inorganic materials are two types of materials with different properties, the particle size of silica sol particles is small, the specific surface area is large, and they are easy to agglomerate. Therefore, it is necessary to carry out certain operations to achieve the combination of both. Silane coupling agent is a kind of reagent commonly used in coupling mixing. Its molecular structure is generally Y-R-Si(OR)_3 , where Si(OR) represents the siloxane oxygen group, the siloxane oxygen group can be connected to an inorganic substance, Y represents an organic functional group, and the organic functional group can be connected with an organic substance. The coating base material investigated in this paper uses pure acrylic emulsion as the organic raw material and silica sol as the inorganic raw material. After the silica sol and the silane coupling agent are mixed and stirred, the silane group at one end of the silane coupling agent can react with the silanol group on the surface of the silica sol particles and then added to the pure acrylic emulsion. The C=C at the other end of the silane coupling agent can be polymerized with the pure acrylic emulsion, which plays a “bridge” role between the two, finally forming a stable system of pure acrylic emulsion-silane coupling agent-silica sol. The mechanism of modification of the silane coupling agent is shown in Figure 2. When the coating is brushed, the water in the coating evaporates and the silica sol particles dehydrate to form Si-O bonds, which are connected into a network to form a Si-O bond three-dimensional structural skeleton with stable and solid structure. The pure acrylic emulsion develops a continuous and even coating thanks to its good film formation and strong plasticity. In short, the pure acrylic emulsion molecules have high flexibility, easy deformation and fusion, and good continuous film forming performance, which improves the brittle cracking and pulverization properties of the silica sol coating, finally forming a continuous, uniform coating. The silica sol particles have small particle size and strong permeability, which can be filled between the molecules of pure acrylic emulsion to form silicon-oxygen bonds, improve crosslinking density, make the coating dense and hard, and improve weather resistance and staining durability to produce organic/inorganic composite coatings in a way that takes full advantage of the benefits of both.

2.2 Preparation of multifunctional coating

According to the expected functions and application requirements of coating materials, the raw materials for functional coatings are divided into three categories: the first category is the main film-forming material, which refers to the main component of the coating and plays a role in stabilizing the adhesive bond. The second category is the secondary film-forming material, which refers to the raw materials that give the coating a specific function, such as pigments and fillers, heat-insulating fillers, etc. The third category is the film-forming auxiliary material, which refers to the auxiliary material to improve the coating function or speed up the preparation process during the coating preparation process.

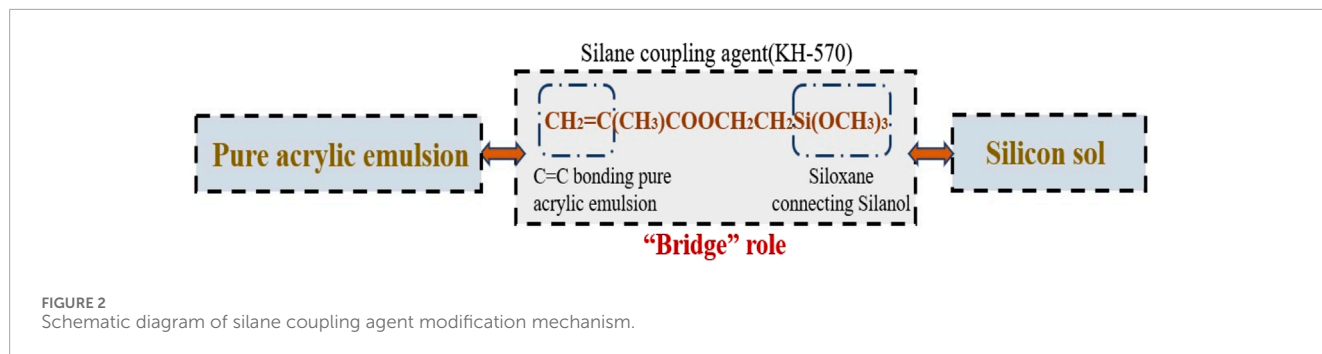


TABLE 1 Main index parameters of materials.

Pure acrylic emulsion	Viscosity/mPa·s	Solid content/%	PH	Residual monomer	Refractive index
	100–500	50	9–10	0.5	1.45–1.50
Silica sol	Grain size/nm	Solid content/%	PH	Metal impurity/ppm	
	15–30	19–20	6.5–8.0	<1	
Silane coupling agent KH-570	Density(g/cm ³)	Purity/%	Molecular weight		Refractive index
	1.04–1.06	≥97	248.4		1.43–1.44
TiO ₂	Relative density(g/cm ³)	Grain size/nm	Molecular weight		Refractive index
	4.2	200–300	79.8		2.76
Hollow microbeads	Bulk density	Grain size/nm	Compressive strength/(kg/cm ³)		Melting point/°C
	0.9–1.2	1–10	4,000–7,000		1,450
Carbon black	Specific surface area/(m ² /g)		Ash/%	Grain size/nm	Density(g/cm ³)
	200–600		≤0.3	9–17	2.1
Dispersant	Active ingredient ratio/%		PH		Viscosity/Pa·s
	40–42		7–8		300

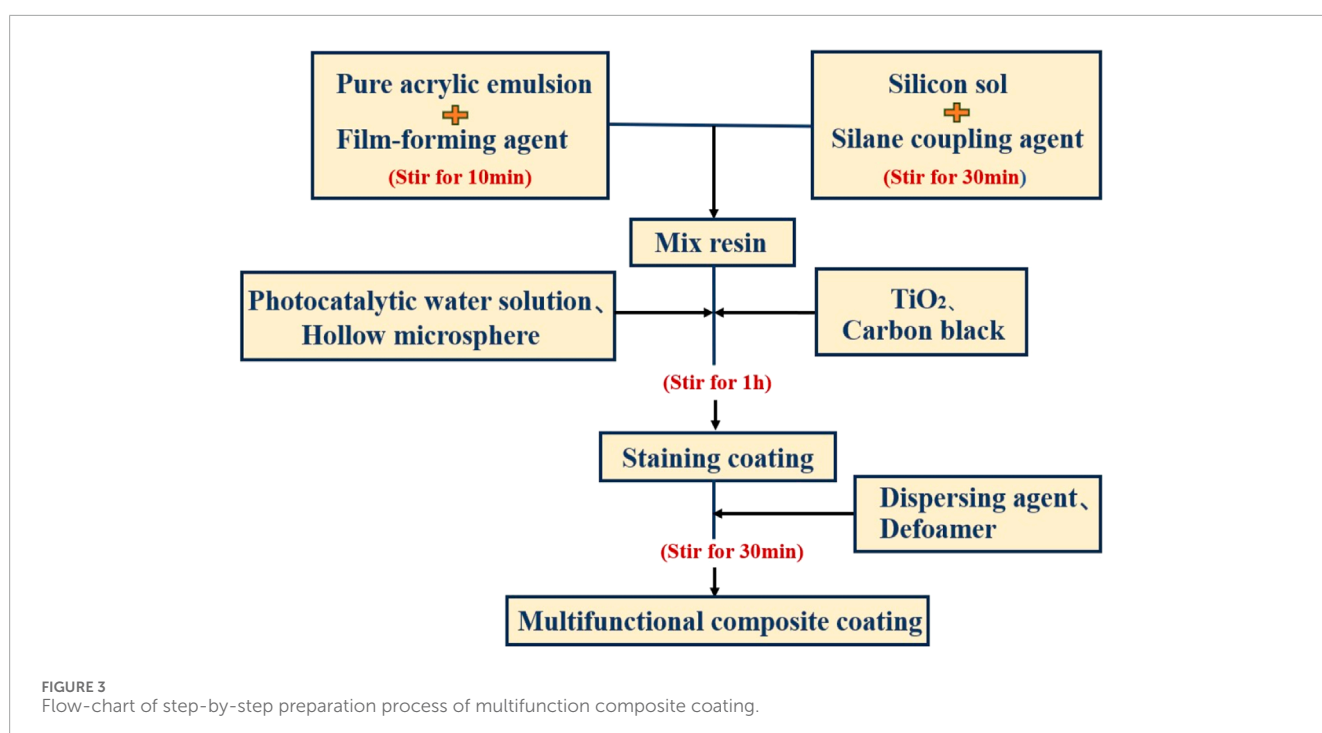
Finally, the composition of the functional coating material in this paper is determined as follows: (1) Main film-forming materials: pure acrylic emulsion, silica sol, silane coupling agent KH-570; (2) Secondary film-forming substances: carbon black, rutile titanium dioxide, hollow microspheres; (3) Film-forming auxiliaries: catalytic aqueous solution as solvent, defoamer, film former, dispersant. The main index parameters of the coating material are listed in Table 1. In order to achieve the best application effect of functional coatings, this article attempts to achieve the best organic/inorganic mass ratio of 2:3 and silica sol particle size of 15 nm. In addition, the carbon black in the coating can cause the color of the coating to become gray to prevent glare and improve the visual effect. However, the amount of carbon black should not be too high and the cooling effect of the road surface should be ensured while avoiding glare. Based on this, three groups of functional coatings with different carbon black content and a blank control group were designed to

compare their functionality. The blend design of each coating is shown in Table 2.

The volume concentration of TiO₂ refers to the percentage of the volume of titanium dioxide volume in the titanium dioxide and in the volume of the mixed base material. The amount of carbon black, hollow microspheres, catalytic aqueous solution, defoamer and dispersant refers to the percentage of the mass of each component to the mass of the mixed base material. The amount of silane coupling agent refers to the mass ratio of the coupling agent to silica sol. The amount of film-forming agent refers to the mass ratio of film-forming agent to pure acrylic emulsion. G0 represents the blank control group without coating. In addition, the ratio of the catalytic aqueous solution was designed as deionized water: silane coupling agent: titanium dioxide: activated carbon: dispersant = 100: 5: 2: 2: 1. The manufacturing process of the final multifunctional coating is shown in Figure 3.

TABLE 2 Coating mix proportion design.

NO.	Organic/inorganic	The volume concentration of TiO ₂	Carbon black/%	Silane coupling agent/%	Hollow microsphere/	Catalytic aqueous solution/%	Film-forming agent/%	Dispersant/%	Defoamer/%
G0	-	-	-	-	-	-	-	-	-
G1	2:3	15	0.6	5	15	20	1	1	0.3
G2	2:3	15	0.9	5	15	20	1	1	0.3
G3	2:3	15	3.6	5	15	20	1	1	0.3



2.3 Experimental methods

2.3.1 Indoor tests

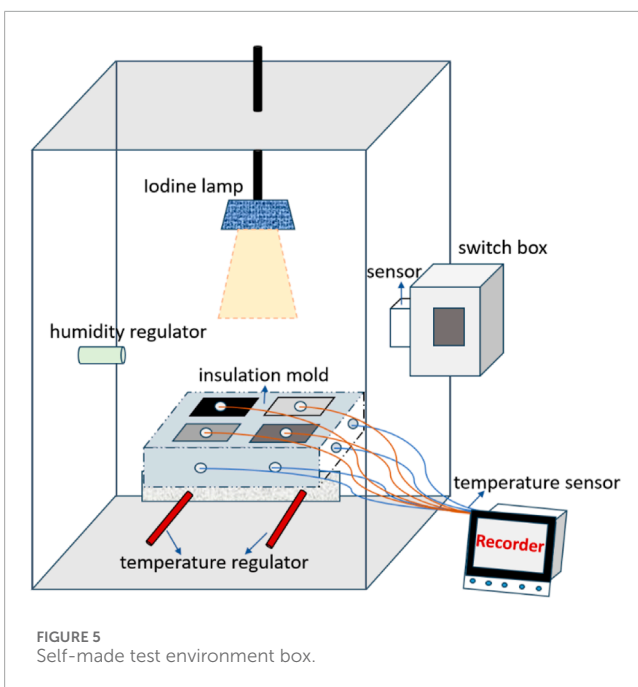
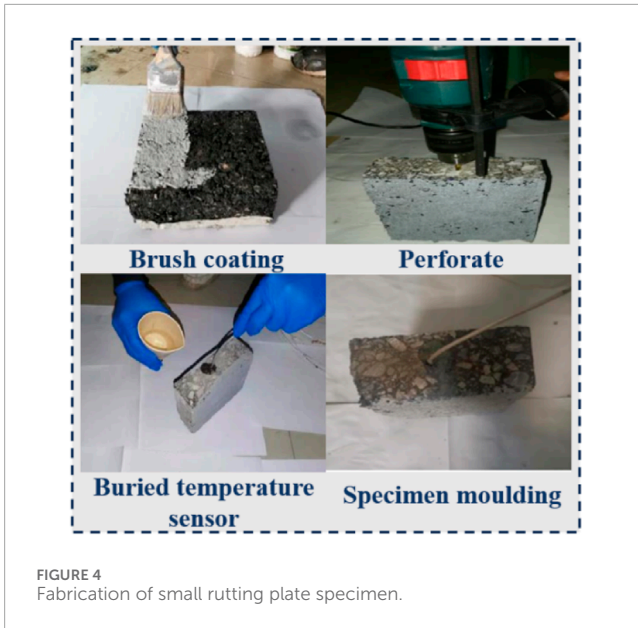
2.3.1.1 Preparation of coated rutting plate specimen

According to the testing requirements, the rutting plate specimens and sizes in this paper meet the specifications and are stored after the preparation is completed. After the rut plate specimen is cooled and formed, the rut plate is divided into four pieces on average by a cutting machine, with a size of 150 mm × 150 mm × 50 mm, which is used to paint the functional coating. In this paper, based on the different content of carbon black, three groups of different functional coatings and a control group without functional coatings were designed for functional tests: G0 is a non-functional coating; G1 is a functional coating with 0.6% carbon black content; G2 is a functional coating with 0.9% carbon black content; G3 is a functional coating with 3.6% carbon black content. Each rut specimen was coated with a coating amount of 0.6 kg/m². In addition, to facilitate the indoor cooling test, holes were drilled at the centroid point of 25 mm height on the side of each small

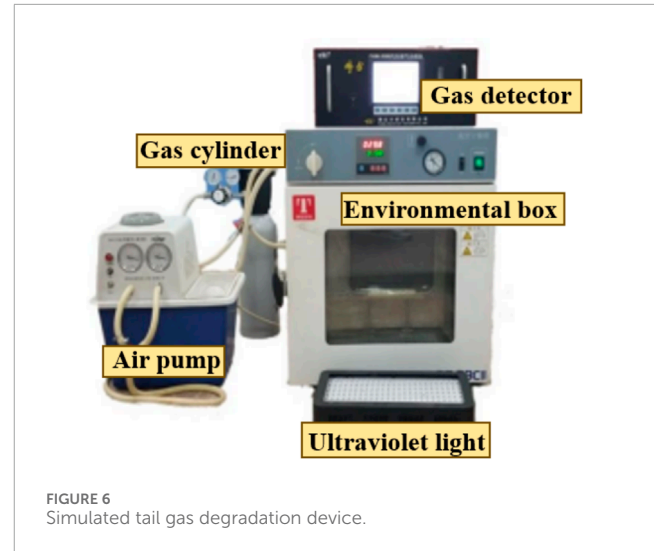
rut plate using an electric drill. The hole diameter was 5 mm and the drilling depth was 75 mm. After drilling was successful, the temperature sensor was implanted into the hole in the center of the specimen. The seal was poured with polyurethane adhesive and the surface was cleaned. The temperature sensor was stuck in the middle of the specimen surface, and then the entire specimen was placed in a self-made insulation mold. The operation process is shown in Figure 4.

2.3.1.2 Indoor cooling test

To make the solar radiation conditions more realistic, this paper created a temperature environment box to simulate the high-temperature outdoor conditions and used an iodine-tungsten lamp as the simulated light source, which is close to the solar radiation spectrum, as well as the power of the iodine. The tungsten lamp is 300 W. To improve the accuracy of the test and the controllability of the variables, the test device should be visualized, which can control the height of the light source, the internal temperature and the humidity. The self-made test device used in this paper



is shown in Figure 5. The temperature and humidity inside the environment box can be controlled. The temperature adjustment range is 0°C–60°C ($\pm 0.5^\circ\text{C}$), the humidity adjustment range is 1%–95% ($\pm 0.5\%$), the accuracy is $\pm 0.5\%$ F.S. and the power supply is 220 V. The specimen can be placed in it to keep it warm, adjust the initial test temperature of the specimen, and improve the accuracy of the test. In addition, other test instruments in this test include a temperature sensor (for collecting temperature information), a paperless recorder (for recording the temperature information collected by a temperature sensor in real time), and a thermal insulation mold (for thermal measurement of rut plate specimens to avoid heat loss). To improve the accuracy of the cooling test, this paper tests the surface temperature and internal temperature



changes of small rutting plate specimens. The pre-prepared G0 to G3 coating rutting plate specimens are placed in the insulation mold in turn and placed directly below the iodine tungsten lamp. At the same time, the temperature sensors inside and on the surface of each specimen are connected to each channel of the paperless recorder to facilitate the recording of temperature data. The test temperature was set at 60°C, the test time was 4 h, and the temperature data after each 30-min interval was used to analyze the cooling effect.

2.3.1.3 Indoor exhaust gas degradation test

The test device for indoor exhaust gas degradation consists of four parts: an ultraviolet lamp, gas bottle, exhaust gas degradation environment box, and gas detector. The test device is shown in Figure 6. The light source wavelength of the ultraviolet lamp is 395 nm, and the radiation intensity of the specimen is 5 mW/cm². The gas composition in the gas bottle is the composition of simulated automobile exhaust, and the specific composition and concentration are shown in Table 3. The environment box adopts the DZ-2BCII vacuum drying box produced in Shandong, which can provide a dry, constant temperature and vacuum test environment for the test. The light source is a 395 nm ultraviolet lamp. The gas detection instrument adopts the FASM-5000 analyzer produced by Foshan Analyzer Co., Ltd., and its main parameters are shown in Table 4. The test environment was maintained at about 30°C and the test time was 2 h. The evaluation method of photocatalytic degradation efficiency is based on Eq. 1.

$$\eta = \frac{C_0 - C_1}{C_0} \times 100\% \quad (1)$$

Where η is the simulated exhaust gas degradation efficiency, C_0 is the initial simulated exhaust gas concentration in an environmental chamber, and C_1 is the simulated exhaust gas concentration after detection in the environmental chamber.

2.3.2 Outdoor tests

Because there is no real simulation of solar radiation in the indoor test, and the conditions such as wind speed and space are constant, the actual environment of the project cannot be truly

TABLE 3 The composition and concentration of simulated gas.

Exhaust gas composition	Concentration	Pressure (MPa)	Volume (L)	Filling gas
CO	8.04%v	10	4	
C ₃ H ₈	0.20%	10	4	N ₂
NO	0.41%v	10	4	

reflected. Therefore, to test the use effect of the multifunctional coating, this paper carries out outdoor tests. The test site is selected in the test section of a section of a sluiceway of an expressway. Based on the indoor test of multifunctional coating, it is found that among the three groups of functional coatings designed, the color of the functional coating group (G1) with 0.6% carbon black content is white, which will affect the driving safety in the actual road surface. Therefore, the outdoor test in this paper will no longer test the functionality of G1, and the test group is proposed as G0, G2, and G3. G2 and G3 coatings were prepared according to the mix ratio of indoor functional coatings and brushed onto the surface of the test section for subsequent functional tests.

2.3.2.1 Outdoor cooling test

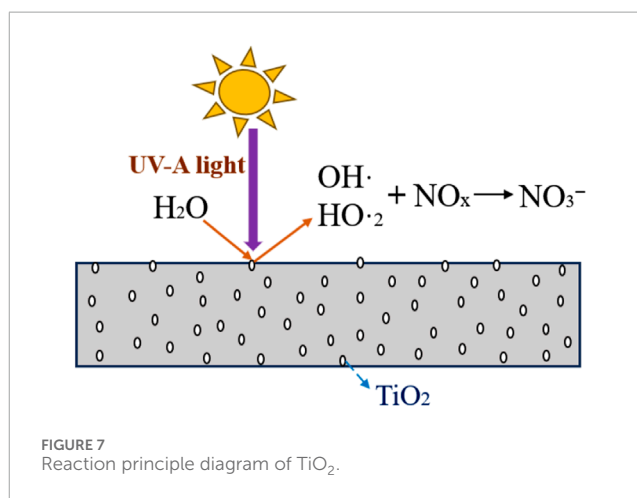
The detection of outdoor temperature includes two parts: road surface and road interior. Among them, the surface temperature of the road surface is detected by an infrared thermometer; the temperature inside the road is detected by a temperature sensor. In this paper, the temperature sensor is embedded in the road before the asphalt surface is paved to achieve the test of the internal temperature of the structure. To avoid damage to the temperature sensor during the paving and rolling process of the asphalt mixture, the temperature sensor is buried and fixed by asphalt mortar, which can effectively improve the success rate of embedding. Among them, the asphalt mortar is calculated and prepared by the equivalent asphalt content in the asphalt mixture.

2.3.2.2 Outdoor exhaust gas degradation test

Photocatalysts can convert the light energy of nature into chemical energy, thereby promoting photocatalytic reactions (Zhao et al., 2022). The reaction principle is mainly to convert the water and oxygen molecules in the surrounding environment into free negative ions with strong oxidation ability, to achieve the purpose of catalytic decomposition of harmful substances. The specific reaction principle is shown in Figure 7. Based on this principle, the outdoor exhaust gas degradation test in this paper compares the exhaust gas degradation effect of each test group by collecting the concentration of nitrate ions produced by the reaction between the coating and the exhaust gas under the condition of solar illumination by industrial distilled water. The specific test methods are as follows: Take an area in each of the three groups of test sections, and use the sealant to form a 20 cm × 20 cm square area in each area. Each square area was cleaned with water once. After drying, the exhaust gas was sprayed with the tail vent of the car towards the square area for 5 min, and then an appropriate amount of distilled water was poured into the square area. After waiting for 3 min, the distilled water was collected into a sealed bottle. Finally,

TABLE 4 Main technical parameters of FASM-5000 analyzer.

Gas	Range	Relative error (%)	Absolute error
H	(0–2,000) × 10 ⁻⁶ vol	±3	±4 × 10 ⁻⁶ vol
C	(0.00–10.00) × 10 ⁻² vol	±3	±0.02 × 10 ⁻² vol
C	(0.0–16.0) × 10 ⁻² vol	±3	±0.3 × 10 ⁻² vol
N	(0–4,000) × 10 ⁻⁶ vol	±4	±25 × 10 ⁻⁶ vol
O	(0.00–25.0) × 10 ⁻² vol	±5	±0.1 × 10 ⁻² vol



the concentration of nitrate ions in the collected distilled water was detected.

2.3.3 Slip resistance test

The anti-sliding performance of the road surface characterizes the ability of the road surface to resist rutting and slip and is an important indicator of the degree of safety of the vehicle. For road coating materials, skid resistance is a common problem. The coating is brushed to the surface of the road to form a coating film, and the surface is smooth. This has changed the original surface characteristics of the road surface, changed the interface

state between the wheel and the road surface, and has a bad impact on traffic safety. Therefore, the study of coating materials for road engineering must consider the skid resistance of the road surface and meet the requirements of the specification indicators. In addition, the thickness of the coating has a direct impact on the skid resistance of the pavement. The thicker the coating, the worse the skid resistance and the lower the driving safety. Therefore, the control of the coating thickness is particularly important. In this paper, the anti-skid performance test is carried out by the pendulum value method, and the test instrument is the pendulum friction instrument. At the same time, the coating thickness is controlled by selecting the coating amount. In this paper, the coating amount of 0.6 kg/m^2 is selected and the coating is evenly applied to the surface of the rutting specimen. The rutting test piece with a coating amount of 0.6 kg/m^2 per unit area was compared with the ordinary test piece. Each test piece was tested at three points, and the average value was finally taken for statistics. According to the 'Highway Subgrade and Pavement Field Test Regulations' (JTG E60-2008), the pendulum value of 45BPN is considered to be qualified.

3 Results and discussion

3.1 Indoor cooling test

Figure 8 shows that the surface temperature of each group increases with the extension of time in the condition of high-temperature test at 60°C , which is due to the temperature rise caused by the absorption of simulated light source radiation heat by the specimen. The slope of each point on the temperature curve generally shows a gradual decrease trend, and the curve tends to be gentle. It can be seen that the heating rate is gradually decreasing and tends to be in a thermal equilibrium state. While Figure 9 shows the internal temperature at 60°C with time, and the trend of curve is similar to that of Figure 8. Overall the temperature of internal is lower than the surface. This is due to the fact that the road surface reflects and blocks some of the heat to the interior of the road. By comparing with the control group G0 without coating, the temperature and heating rate of the specimen with functional coating are lower than those without coating, indicating that the functional composite coating has a cooling effect. By comparing three groups of functional coatings (G1~G3) with different carbon black content, it was found that with the increase of carbon black content, the cooling effect showed a downward trend, that is, the cooling effect was $G1 > G2 > G3$, which indicated that the increase of carbon black content reduced the reflection effect of titanium dioxide on solar radiation to a certain extent, thus weakening the cooling effect of the coating. From the data point of view, the surface cooling of each functional coating specimen: G1 cooling 5.8°C , G2 cooling 5.4°C , G3 cooling 4.7°C ; the internal cooling of each functional coating specimen: G1 cooling 4.8°C , G2 cooling 4.3°C and G3 cooling 3.8°C . In summary, the functional coating has a certain cooling effect under high-temperature conditions. At the same time, with the increase of carbon black content, the cooling effect of the functional coating decreased, but the decrease was not too large. Therefore, the content of carbon black can be selected

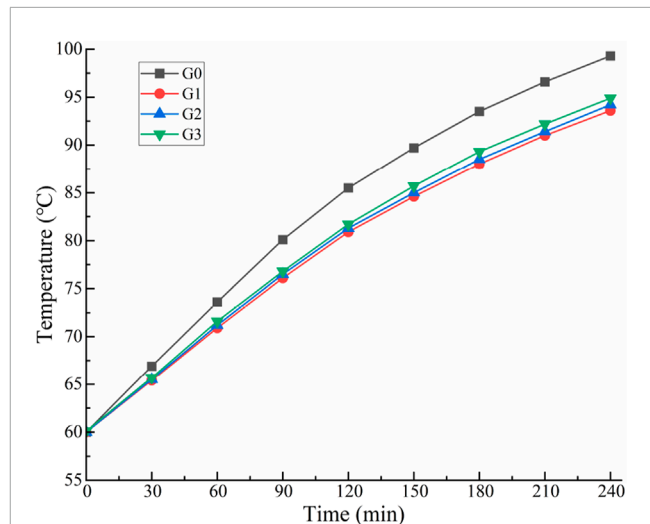


FIGURE 8
Variation of surface temperature (at 60°C) with time.

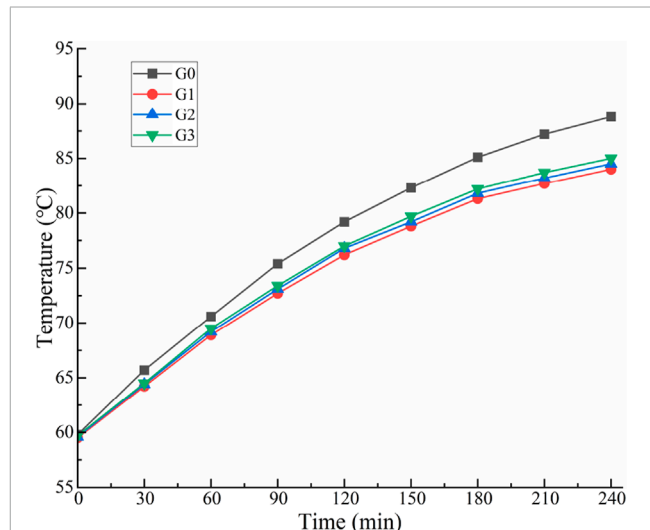
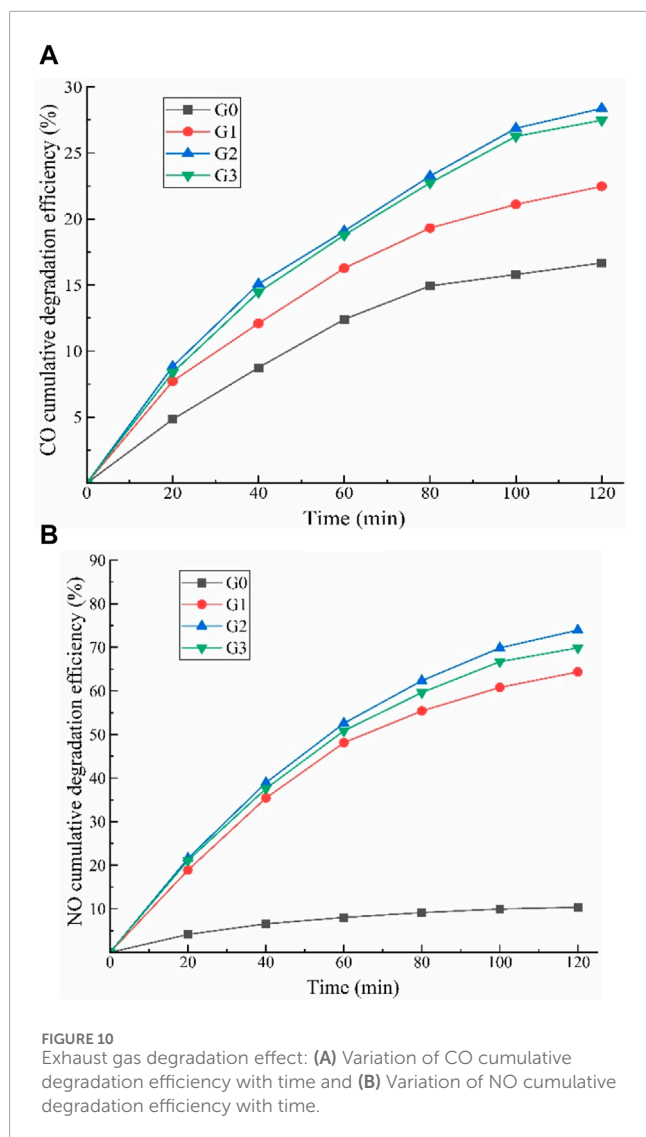


FIGURE 9
Variation of internal temperature (at 60°C) with time.

according to the comprehensive consideration of the cooling effect and visual effect.

3.2 Indoor exhaust gas degradation effect

Figure 10 shows that the functional coating group has a good effect on the degradation of automobile exhaust, and the degradation efficiency of the exhaust gas is higher at the beginning of the test, but the degradation efficiency gradually decreases with the increase of time, and the part after the curve shows a gentle trend. Compared with CO, the degradation effect of functional coatings on NO is more prominent, and the cumulative degradation efficiency of NO in G1 to G3 is much higher than that in G0. In addition, by comparing the exhaust gas degradation effect of three groups of functional coating



groups with different carbon black content, the results show that the degradation effect from high to low is: G2 > G3 > G1, that is, the best degradation ability is G2. The cumulative degradation efficiency of CO was 27.77%, and the cumulative degradation efficiency of NO was 73.75%.

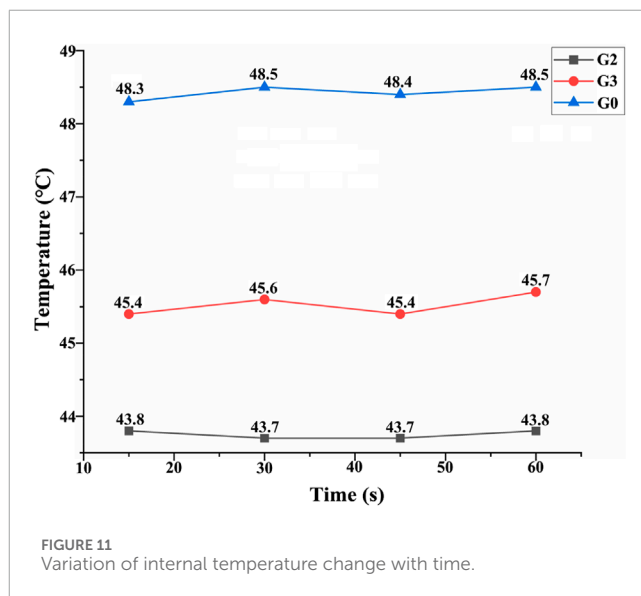
3.3 Outdoor cooling test

The surface temperature and internal temperature of the three test groups were tested at the same period, and the temperature of each measuring point was measured four times at an interval of 15 s in 1 minute. Because the surface temperature test is greatly affected by the surrounding environment, the average of the four temperatures measured on the surface is taken as the surface temperature of the period. The measured surface temperature and internal temperature data are collated in Table 5; Figure 11, respectively.

It can be calculated from the data results of Table 5 and Figure 11 that the difference between the surface temperature and the internal

TABLE 5 Surface temperature change.

Number	G0	G2	G3
Surface temperature (°C)	49.2	46.5	48



temperature of G0 in the non-coating group is 0.72°C. The difference between the road surface temperature and the internal temperature of G2 and G3 in the functional coating group was 2.75°C and 2.48°C, respectively. It can be seen that the functional coating has a good heat reflection effect, thereby reducing the heat absorption of some road surfaces and transmitting it to the interior of the structure. In addition, compared with the control group G0 without coating, it was found that the surface temperature of the functional coating group G2 decreased by 2.7°C, and the internal temperature decreased by 4.7°C. The surface temperature of G3 decreased by 1.2°C, and the internal temperature decreased by 1.9°C. In summary, the functional coating group G2 has better cooling capacity.

3.4 Outdoor exhaust gas degradation effect

By collecting the collected distilled water to determine the nitrate ion concentration, the detailed test results are shown in Table 6. According to the reaction mechanism of TiO₂ in Figure 7, the catalytic degradation effect of photocatalyst (TiO₂) in functional coatings is proportional to concentration of nitrate ions, that is, the higher the concentration of nitrate ions, the better the degradation effect of the exhaust gas. Therefore, it can be seen from Table 6 that the concentration of nitrate ions in G2 and G3 in the functional coating group is higher than that in the uncoating control group G0, indicating that compared with the ordinary pavement, the pavement with functional coating has a certain ability to reduce exhaust gases. In addition, for the functional coating group with different carbon black content, the nitrate ion concentration of G2 is higher than

TABLE 6 NO₃⁻ concentration detection result.

Number	Time/min	Peak area/ $\mu\text{S} \cdot \text{min}$	Peak height/ μS	NO ₃ ⁻ concentration
G0	9.75	0.14	0.58	1.13
G2	9.75	0.3	1.29	2.17
G3	9.75	0.15	0.62	1.18

TABLE 7 Pendulum test result.

Coating amount/(kg/m ²)	First/BPN	Second/BPN	Third/BPN	Pendulum value/BPN
0	79	70	71	73
0.6	60	58	63	60

that of G3, indicating that G2 with 0.9% carbon black content has a stronger exhaust gas degradation effect.

3.5 Slip resistance test

Through the pendulum value test of the two specimens, the result is shown in Table 7.

From the test results in Table 7, it can be seen that the pendulum values of the two specimens are greater than 45 BPN, which meets the requirements of the specification and has passed the anti-slip performance test. On the whole, the slip resistance value of the rutting specimen with coating is lower than that of the rut pattern without coating. This is because after the coating is applied to the surface of the mixture, part of the coating fills the gap between the surface structure of the asphalt mixture and changes the structure of the specimen. The depth makes the friction between the rubber slider of the pendulum instrument and the surface of the specimen decrease, and the pendulum value decreases. Therefore, when brushing the coating, it is necessary to control the amount of coating while ensuring the cooling effect. When the coating amount is small, the coating is partially filled with the road surface structure, and there are still some areas where the structure is still rough, providing friction. As the coating amount gradually increases, the coating fills the road surface structure of the specimen, and the friction depends on the friction of the coating itself. At this time, the friction provided is low, and the anti-slip performance cannot meet the requirements, which poses a danger to driving safety.

4 Conclusion

The danger posed by high temperature on asphalt surface has always been the focus of road workers. At the same time, environmental pollution caused from car exhaust is also an urgent problem that needs to be solved. To overcome these two main problems, the solutions proposed in the past are mostly "palliative solutions" that do not fundamentally solve the main problems and whose functionality is relatively simple. This article proposes a multifunctional composite coating to achieve a coating on the

surface of the asphalt pavement, which can achieve the effect of cooling and exhaust gas degradation at the same time. It not only controls the material cost but also has a good application. Indoor and outdoor cooling tests and emissions degradation tests are also carried out on multifunctional coatings. The main conclusions of study are summarized as follows:

1. A functional composite coating with cooling and exhaust gas degradation effects was developed and rutile titanium dioxide and carbon black were used as pigments and fillers in the coating preparation, including titanium dioxide with a certain refractive index and photocatalytic effect. Carbon black is used to balance the color of the coating and avoid glare caused by the excessive white color of the coating, affecting the driver's driving safety. However, the amount of carbon black should not be too high, and the cooling effect of the road surface should be ensured while avoiding glare. In this paper, three types of functional coatings with different carbon black content are examined in order to select an optimal solution in terms of functionality and safety.
2. The results of the indoor test show that in the cooling test, the cooling effect of the multifunctional coating group decreases with the increase in carbon black content. It turns out that G1 with a content of 0.6% achieves the best cooling effect, followed by G2 with a content of 0.9%. However, the cooling rate of G1 is only slightly higher than that of G2. Considering the visual effect, it is considered that G2 is the optimal cooling function coating group. In the exhaust gas degradation test, the multifunctional coating group showed a certain exhaust gas degradation ability, and the degradation efficiency reached a high level at the beginning of the test. The test results show that the degradation effect is from high to low: G2 > G3 > G1. This implies that the functional coating group with the best exhaust gas degradation ability is G2. The cumulative degradation efficiency of CO was 27.77% and the cumulative degradation efficiency of NO was 73.75%.
3. The results of the outdoor tests showed that in the cooling test, the surface temperature of the functional coating group G2e surface temperature of the functional coating group decreased by 2.7°C and the internal temperature decreased by 4.7°C.

The surface temperature of G3 decreased by 1.2°C and the internal temperature decreased by 1.9°C. This shows that G2 has better heat reflection ability and cooling effect. In the exhaust gas degradation test, the NO₃- concentrations detected by G2 and G3 in the functional coating group were 2.17 and 1.18, respectively, indicating that the exhaust gas degradation effect of G2 was stronger than that of G3.

- Based on the results from the functional tests indoors and outdoors, the conclusion is that the functional coating group G2 with 0.9% carbon black content has the best cooling and exhaust gas reduction effect. At the same time, it is concluded from the anti-slip test that the BPN value of the multifunctional coating with a coating amount of 0.6 kg/m² meets the requirements of the specification and ensures road safety.

Data availability statement

The original contributions presented in the study are included in the article/Supplementary Material, further inquiries can be directed to the corresponding author.

Author contributions

PH: Conceptualization, Investigation, Writing–original draft. FC: Methodology, Writing–original draft. MC: Conceptualization, Writing–review and editing. XG: Conceptualization, Data curation, Writing–review and editing. XH: Data curation, Formal Analysis,

Methodology, Writing–original draft. YJ: Supervision, Validation, Writing–review and editing. ZL: Formal Analysis, Validation, Writing–review and editing.

Funding

The author(s) declare financial support was received for the research, authorship, and/or publication of this article. The study was supported by the National Natural Science Foundation of China (Grant No: 51778071).

Conflict of interest

Authors PH, FC, and MC were employed by Guangzhou Expressway Company.

The remaining authors declare that the research was conducted in the absence of any commercial or financial relationships that could be construed as a potential conflict of interest.

Publisher's note

All claims expressed in this article are solely those of the authors and do not necessarily represent those of their affiliated organizations, or those of the publisher, the editors and the reviewers. Any product that may be evaluated in this article, or claim that may be made by its manufacturer, is not guaranteed or endorsed by the publisher.

References

- Brouwers, Q. L. Y. J. H. (2009). Indoor air purification using heterogeneous photocatalytic oxidation. Part I: experimental study. *Appl. Catal. B Environ.* 92, 454–461. doi:10.1016/j.apcatb.2009.09.004
- Cheng, R., Liang, Q. O., and Lin, D. G. (2020). Quantitative risk evaluation for late rice: hazard factors in Zhejiang province, China. *Geomatics Nat. Hazards Risk* 11 (1), 786–802. doi:10.1080/19475705.2020.1748726
- Chulkov, A. O., Vavilov, V. P., and Moskovchenko, A. I. (2019). Active thermal testing of delaminations in heat-shielding structures. *Russ. J. Nondestruct. Test.* 55 (3), 240–247. doi:10.1134/S1061830919030033
- Cui, S. C., Xie, B. W., Li, R., Pei, J. Z., Tian, Y. F., Zhang, J. P., et al. (2020). g-C₃N₄/CeO₂ Binary composite prepared and its application in automobile exhaust degradation. *Materials* 13 (6), 1274. doi:10.3390/ma13061274
- Dalapati, G. K., Masudy-Panah, S., Chua, S. T., Sharma, M., Wong, T. I., Tan, H. R., et al. (2016). Color tunable low cost transparent heat reflector using copper and titanium oxide for energy saving application. *Sci. Rep.* 6, 20182. doi:10.1038/srep20182
- Debbage, N., and Shepherd, J. M. (2015). The urban heat island effect and city contiguity. *Comput. Environ. Urban Syst.* 54, 181–194. doi:10.1016/j.compenurbysys.2015.08.002
- Du, Y. F., Dai, M. X., Deng, H. B., Wei, T. Z., and Li, W. (2020). Evaluation of thermal and anti-rutting behaviors of thermal resistance asphalt pavement with glass microsphere. *Constr. Build. Mater.* 263, 120609. doi:10.1016/j.conbuildmat.2020.120609
- Gao, X. F., Sun, Z. H., Ma, J. P., Chen, W. X., Shang, S. M., and Chiu, K. L. (2023). Synthesis of the solar heat reflecting membrane by duplicating the Saharan silver ant micro-hair structure. *Colloid Polym. Sci.* 301, 1239–1246. doi:10.1007/s00396-023-05146-6
- Geng, J. G., Chen, M. Y., Shang, T., Li, X., Kim, Y. R., and Kuang, D. L. (2019). The performance of super absorbent polymer (SAP) water-retaining asphalt mixture. *Materials* 12 (12), 1964. doi:10.3390/ma12121964
- Gong, X., Liu, Q. T., Lv, Y., Chen, S. C., Wu, S. P., and Ying, H. (2020). A systematic review on the strategies of reducing asphalt pavement temperature. *Case Stud. Constr. Mater.* 18, e01852. doi:10.1016/j.cscm.2023.e01852
- Guntor, N. A. A., Fadhil, M., Ponraj, M., and Iwao, K. (2014). Thermal performance of developed coating material as cool pavement material for tropical regions. *J. Mater. Civ. Eng.* 26 (4), 755–760. doi:10.1061/(ASCE)MT.1943-5533.0000859
- Jiang, W. Q., and Yu, C. S. (2020). Application of environmentally friendly nanomaterials based on nitrogen oxide catalytic purification of automobile exhaust. *Int. J. Nanotechnol.* 17 (2-6), 375–392. doi:10.1504/IJNT.2020.110724
- Kang, S., Lee, D., Park, J., and Jung, J. (2022). Exploring urban forms vulnerable to urban heat islands: a multiscale analysis. *Sustainability* 14 (6), 3603. doi:10.3390/su14063603
- Kia, A., Delens, J. M., Wong, H. S., and Cheeseman, C. R. (2021). Structural and hydrological design of permeable concrete pavements. *Case Stud. Constr. Mater.* 15, e00564. doi:10.1016/j.cscm.2021.e00564
- Lei, W. M. Z. (2010). *Composite based long-life asphalt pavement analysis*.
- Lin, M. F., Tang, J., and Liu, M. (2019). Sponge city planning of dalian based on functional division of natural ecological environment. *EKOLOGI* 28 (107), 3557–3567.
- Liu, Y., Li, T., and Peng, H. Y. (2018). A new structure of permeable pavement for mitigating urban heat island. *Sci. Total Environ.* 634, 1119–1125. doi:10.1016/j.scitotenv.2018.04.041
- Mathew, A., Khandelwal, S., and Kaul, N. (2018). Analysis of diurnal surface temperature variations for the assessment of surface urban heat island effect over Indian cities. *Energy Build.* 159, 271–295. doi:10.1016/j.enbuild.2017.10.062
- Maurly-Ramirez, A., De Muynck, W., Stevens, R., Demeestere, K., and De Belie, N. (2013). Titanium dioxide based strategies to prevent algal fouling on cementitious materials. *Cem. Concr. Compos.* 36, 93–100. doi:10.1016/j.cemconcomp.2012.08.030
- Shimazaki, Y., Aoki, M., Karaki, K., and Yoshida, A. (2022). Improving outdoor human-thermal environment by optimizing the reflectance of water-retaining

pavement through subjective field-based measurements. *Build. Environ.* 210, 108695. doi:10.1016/j.buildenv.2021.108695

Si, C. D., Cao, H., Chen, E. L., You, Z. P., Tian, R. L., Zhang, R., et al. (2018). Dynamic response analysis of rutting resistance performance of high modulus asphalt concrete pavement. *Appl. Sciences-Basel* 8 (12), 2701. doi:10.3390/app8122701

Si, W., Yin, Y. K., Hu, Y. P., Kang, X. X., Xu, Y. S., Shi, A. Y., et al. (2022). Analysis on factors affecting the cooling effect of optical shielding in pavement coatings. *Build. Environ.* 211, 108766. doi:10.1016/j.buildenv.2022.108766

Suszanowicz, D., and Kolasa-Wieczek, A. (2019). The impact of green roofs on the parameters of the environment in urban areas-review. *Atmosphere* 10 (12), 792. doi:10.3390/atmos10120792

Synnefa, A., Karlessi, T., Gaitani, N., Santamouris, M., Assimakopoulos, D. N., and Papakatsikas, C. (2011). Experimental testing of cool colored thin layer asphalt and estimation of its potential to improve the urban microclimate. *Build. Environ.* 46 (1), 38–44. doi:10.1016/j.buildenv.2010.06.014

Wang, X. H., Wu, Y., Gong, J., Li, B., and Zhao, J. J. (2019). Urban planning design and sustainable development of forest based on heat island effect. *Appl. Ecol. Environ. Res.* 17 (4), 9121–9129. doi:10.15666/aecr/1704_91219129

Wang, Y. F., Bakker, F., de Groot, R., and Wortche, H. (2014). Effect of ecosystem services provided by urban green infrastructure on indoor environment: a literature review. *Build. Environ.* 77, 88–100. doi:10.1016/j.buildenv.2014.03.021

Xu, Y., Chen, W., Jin, R. Y., Shen, J. S., Smallbone, K., Yan, C. Y., et al. (2018). Experimental investigation of photocatalytic effects of concrete in air purification adopting entire concrete waste reuse model. *J. Hazard. Mater.* 353 (JUL.5), 421–430. doi:10.1016/j.jhazmat.2018.04.030

Zhang, H., Quan, W., Liu, J., and Lai, F. (2020). Thermosetting powder coating for asphalt pavement. *Road Mater. Pavement Des.* 21 (1), 217–236. doi:10.1080/14680629.2018.1484383

Zhang, H. T., Gong, M. Y., and Liu, Z. Q. (2022). Study on thermal resistance efficiency of open-graded frictional course pavements bad on a laboratory simulated test. *Int. J. Pavement Eng.*,

Zhang, S. S., Zhang, Z. Q., Pei, J. Z., Li, R., Zhang, J. P., Cai, J., et al. (2018). A novel TiO₂-SiO₂ aerogel nanocomposite absorbent: preparation, characterization and photocatalytic degradation effects on automobile exhaust. *Mater. Res. Express* 5 (2), 025036. doi:10.1088/2053-1591/aaaf10

Zhao, H. Y., Jia, B. N., Guan, X. N., Chen, Y. J., Zhu, X. L., Han, L. H., et al. (2022). A promising type-II β -AsP/g-C₆N₆ van der Waals heterostructure photocatalyst for water splitting: a first-principles study. *Phys. Chem. Chem. Phys.* 24 (40), 24939–24949. doi:10.1039/d2cp03247c